Near-Surface Velocity Variability at Inertial and Subinertial Frequencies in the Vicinity of the California Current*

ROBERT A. WELLER

Woods Hole Oceanographic Institution, Woods Hole, MA 02543

(Manuscript received 5 July 1984, in final form 8 January 1985)

ABSTRACT

Observations of the horizontal velocity field in the upper 150 m, made from the Research Platform FLIP as it drifted off the coast of Baja California, were used to examine the variability of the velocity field and its relation to local wind forcing. At subinertial frequencies a spatially varying flow field associated with the California Current System was encountered. In addition, there was low frequency near-surface flow to the right of the wind stress that decayed with depth. At near-inertial frequencies oscillatory motion with an amplitude of up to 40 cm s^{-1} was observed. Most of the energy in the near-inertial frequency band was associated with modes with vertical wavelengths large compared to the thickness of the mixed layer. The local wind alone had neither the strength nor the variability needed to directly produce the observed inertial period variability. It is suggested that FLIP encountered regions in which the shear of the quasi-geostrophic flow resulted in localized intensifications of near-inertial motion.

1. Introduction

In this paper a recent set of velocity observations taken in the upper 150 m of the ocean in the vicinity of the California Current is presented. The horizontal velocity data were collected from the Research Platform FLIP as it drifted off the coast of Baja California in April and May of 1980. Local winds and other meteorological parameters were measured on board FLIP during the experiment. The intent of the experiment was to collect data that would permit investigation of the response of the upper ocean to local atmospheric forcing. With this data we hoped to: 1) identify and study the wind driven component of the velocity field in the upper ocean and, in particular, to study the generation of inertial motions in the mixed layer and below by the wind stress; and 2) to investigate the response of the mixed layer to the combined fluxes of heat and momentum. The data set proved to be very well suited for the study of the second area of interest, and results of that work are presented in Price *et al.* (1985). While pursuing the first area of interest we found that, at subinertial frequencies, the velocity field, though dominated by spatially varying flow associated with the California Current, did have a component that was driven by the local wind. At near-inertial frequencies, however, the data set showed unanticipated velocity variability. The purpose of this paper is to report and discuss the observed velocity variability, with emphasis on that at near-inertial frequencies.

The experiment and methods used to collect the data are summarized in Section 2. An overview of the velocity and temperature data collected in the upper 150 m and a brief discussion of the observed velocity variability are given in Section 3, with a more detailed description of the velocity variability in the near-inertial frequency band provided in Section 4. The near-inertial motions and possible sources of the oscillations are discussed in Section 5. Conclusions are given in Section 6.

2. The experiment and the methods

In late April 1980 the Research Platform FLIP was towed to a site (31°N, 124°W) southwest of San Diego, California. (FLIP was used to provide a stable measurement platform; for a discussion of FLIP's motion see Rudnick, 1967, and Regier, 1975.) From 28 April to 24 May FLIP remained in the vertical position and drifted 250 km to the south (Fig. 1). While FLIP drifted a variety of meteorological and oceanographic measurements were made by the author and by Dr. Robert Pinkel of Scripps Institution of Oceanography (Pinkel, 1983). Meteorological measurements included wind velocity measured 22 m above the sea surface. The winds were light to moderate and typically to the south. Oceanographic measurements were made, with the exception of Pinkel's Doppler sonar measurements, by lowering instrumentation from the end of long booms extending horizontally out from FLIP's hull (Fig. 2). Conduc-

* Woods Hole Oceanographic Institution Contribution Number 5632.

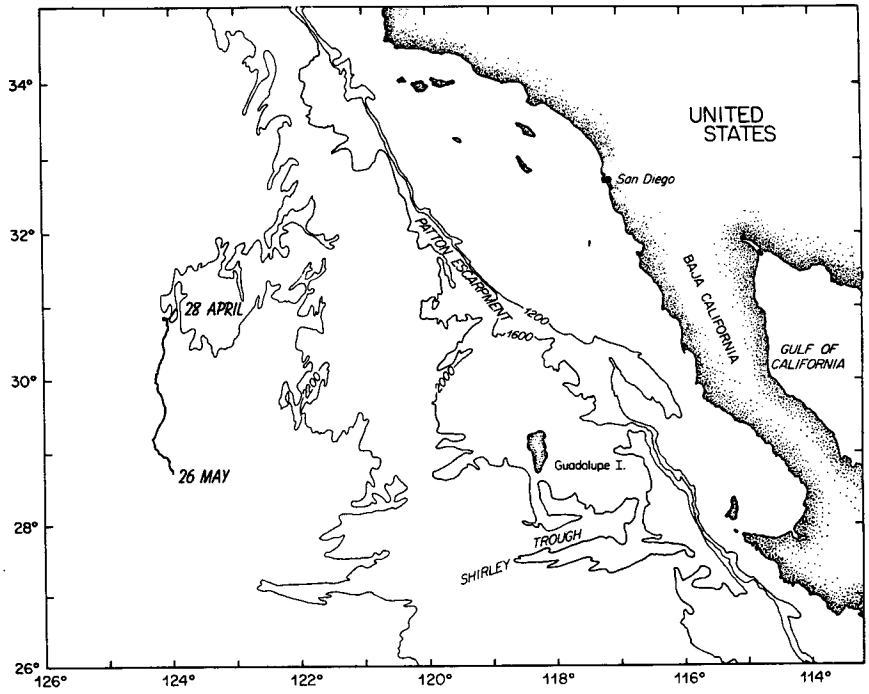

FIG. 1. During the experiment, which began 28 April 1980 and ended 26 May 1980, FLIP drifted south off the coast of Baja California as shown. The depth contours are shown in fathoms.

tivity and temperature measurements were made by Pinkel using instruments that covered the depth range of 4–440 m every two minutes. Temperature and velocity profiles were made by profiling with four Vector Measuring Current Meters. (See Weller and Davis, 1980, for a description of these instruments, hereafter referred to as VMCMs.) The four VMCMs were attached to the wire as two pairs of two instruments and raised and lowered to obtain data over depths from 5–150 m. Within each pair the instruments were separated by 4.5 m; the two pairs were separated by 70 m. A fifth VMCM was suspended at the fixed depth of 2 m for the duration of the experiment. During the experiment an autopilot coupled to a gyro compass maintained FLIP's heading with a propeller thruster. This heading was chosen so that if FLIP was being blown downwind through the water then the current meters hanging from the booms would be in front and to the side of any wake created by the hull.

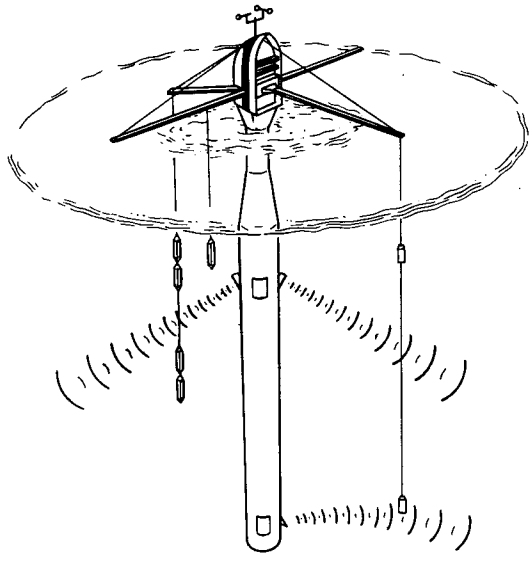

FIG. 2. The Research Platform FLIP as configured for this experiment. Four booms were deployed. CTD profiling was done by Pinkel from one boom; velocity profiling was done from another boom using Vector Measuring Current Meters (VMCMs). A fifth VMCM was held at a fixed depth, suspended from a third boom. Meteorological measurements were made from FLIPs mast, 22 m above the sea surface.

During the experiment FLIP's drift was monitored with a Northstar 6000 Loran C receiver. Latitude and longitude displayed by the Northstar were manually logged every 30 minutes for the duration of the experiment. For approximately 80 percent of the experiment Loran data (latitude, longitude, time delays, signal to noise ratios, and warning codes) were also recorded at rapid sampling intervals by computer. Typically the rate was once per minute, though at times the data was recorded every 15 seconds. During most of the remaining 20 percent of the time the rapidly sampled Loran C data was recorded every minute on a line printer; this data was later entered by hand and merged with the computer record.

The four VMCMs used as profilers were attached

to a torque-balanced stainless steel wire. As the instruments were raised and lowered the wire tended to rotate slowly (approximately one revolution every five minutes) as the tension in it varied. To some extent this tendency was countered by placing a weight beneath the deepest VMCM. In any case, the VMCMs perform, using a compass heading up-dated every second, a vector velocity computation when either of the two orthogonal propellers undergoes ¼ of a revolution (corresponding to approximately a 10 cm displacement of fluid along the axle of the propeller); and the revolution of the instruments on the wire was not a source of significant error in the measurement of horizontal velocity. The VMCMs were used because of their ability to make accurate measurements of low frequency variability when in the presence of vertical flow associated with surface waves or when in the presence of vertical flow associated with slow vertical profiling (Weller, 1978; Davis and Weller, 1980). For this experiment the VMCMs were fitted with external fast response temperature sensors (Rosemount, Inc., platinum resistance thermometers) and pressure transducers (Gould) with 250 psi full scale range.

Current profiling with the VMCMs was an automatic operation. A hydraulic winch was used to raise and lower the instruments, cycling them up and down between two depths. During the descents 76.2 m of wire was payed out at approximately 3.5 m per minute, and the wire was recovered at approximately 2.5 m per minute. During the course of the day the temperature and thus the viscosity of the hydraulic oil used in the motor powering the winch varied, so that the time required to complete one profile varied. To space the start of the profiles evenly in time, the profiling was stopped at the end of each down then up cycle, with the VMCMs resting at their upper limit of travel, until exactly 60 minutes after the beginning of the last profiling cycle. This pause period at the end of each cycle varied between 6 and 10 minutes.

The velocities measured by the VMCMs were recorded as vector-averages over 1 minute. When profiling, the current meters yield a velocity that is averaged over both depth and time. In contrast, the temperature and pressure measurements were instantaneous measurements made at the end of each 1-minute sampling interval. The VMCMs recorded on cassette tape, and sampling was interrupted on 11 May for 64 minutes in order to replace the batteries and cassettes in the current meters.

3. The temperature and velocity fields

The data from the VMCM at 2 m and the four profiling VMCMs were merged by combining all data within plus and minus 2 meters of each of 38 depths [$(2 + 4n)$ meters, where $n = 0, 1, 2, \ldots, 37$] into 38 irregularly spaced time series of u, v and temperature. There were between 1500 and 15000, typically 3000, points in each time series. Linear interpolation was used to create evenly spaced, 712-hour long time series with 30-minute sampling intervals. Figures 3a, b, and c show, respectively, three dimensional representations of the temperature, u velocity component and v velocity component fields.

The mixed layer, shown as the nearly isothermal, near-surface plateau in Fig. 3a, was typically 45 m

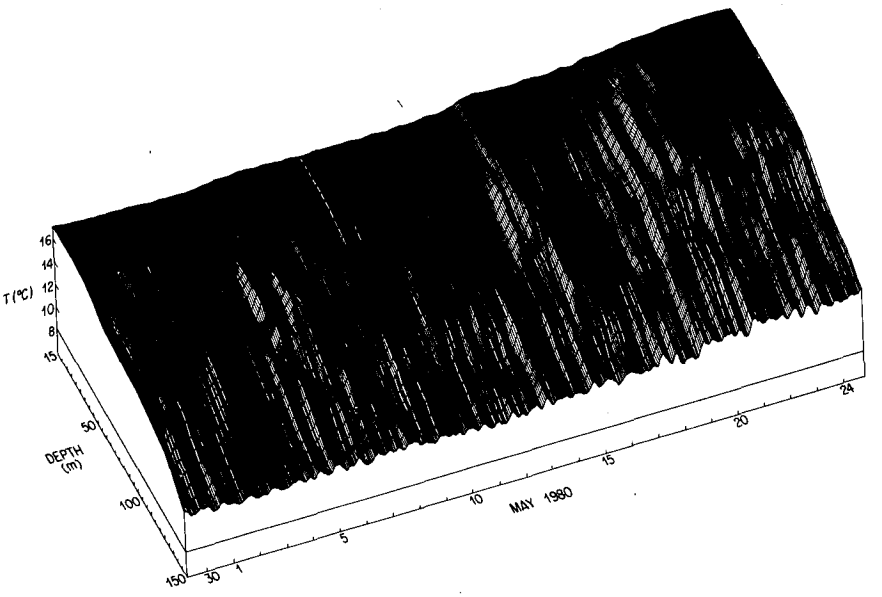

FIG. 3a. Contours of temperature, shown as a function of depth and time. A 5-hour running mean was applied to the data before producing this plot.

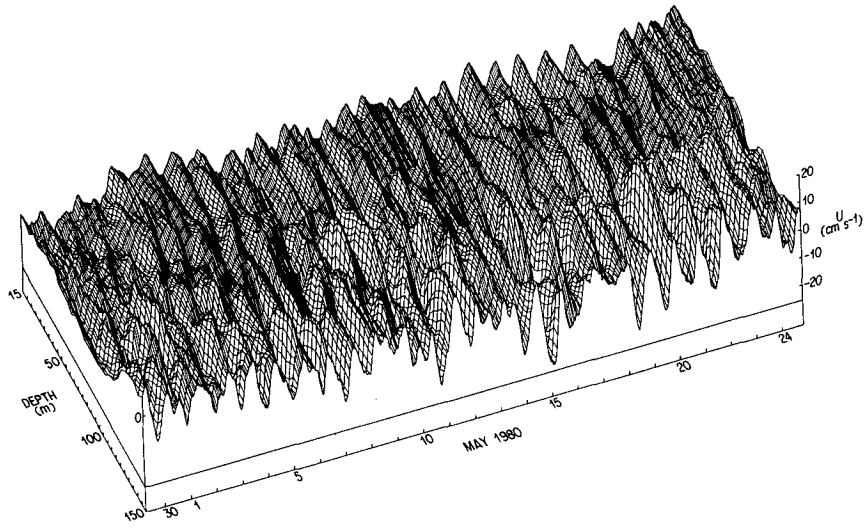

FIG. 3b. Contours of the u velocity component, shown as a function of depth and time. A 5-hour running mean was applied to the data before producing this plot.

deep. On occasion, however, both the mixed layer depth increased abruptly to 70 m and the temperature increased rapidly at all of the 38 depth levels. Figure 4a shows, as an example, the temperature time series from 22 m. The temperature changes on 5–7, 14, and 17–23 May were much larger than those associated with air–sea interaction processes (Price *et al.*, 1985). The CTD data (Fig. 4b) showed that at these times FLIP had entered water that was saltier as well as warmer. Below the base of the mixed layer, there was also semidiurnal period variability associated with the semidiurnal tide (Fig. 5). There was, however, little diurnal period temperature variability found beneath the base of the mixed layer.

To convert the relative velocity data to absolute velocity data it was necessary to produce a time series of FLIP's drift velocity and add the drift velocity to the measured relative velocity. Analysis of the rapidly sampled Loran C data showed considerable variability in FLIP's position. Much of that variability was associated with the performance of the Loran C receiver rather than with actual motion of FLIP. To remove the high frequency noise it was necessary to low pass filter the one minute sampling interval Loran data and then average it to produce a time series of FLIP's drift with a 30 minute sampling interval. This time series was then added to each of the relative velocity time series to create absolute horizontal velocity time series at 38 levels.

There was little depth-averaged mean flow in the relative east–west velocity component, but the relative north–south velocity component had a mean north-

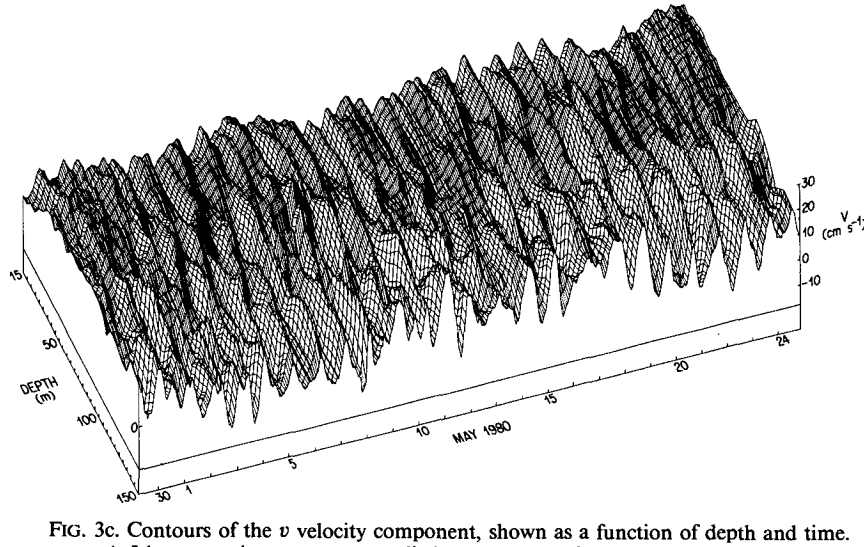

FIG. 3c. Contours of the v velocity component, shown as a function of depth and time. A 5-hour running mean was applied to the data before producing this plot.

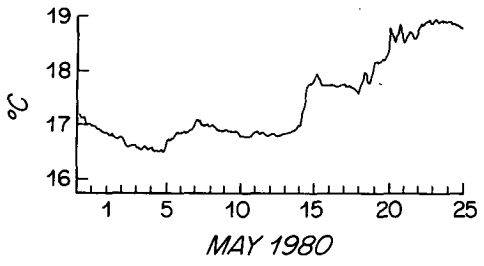

FIG. 4a. Time series of temperature at 22 m.

ward flow. This is associated with FLIP's drift. FLIP drifted to the south under the influence of the southward winds. FLIP's drift velocity averaged 12 cm s^{-1} to the south, while the absolute velocity field had an average southerly component of approximately 5 cm s^{-1}. Though FLIP drifted almost exactly due south along 124°W, the low frequency component of the flow was at various times westward, northward, and southwestward (Fig. 6).

The variability in the subinertial flow field, like that observed in the temperature field, is typical of the highly variable fields found in this region of the California Current system. Lynn and Svejkovsky (1984) presented AVHRR imagery of this area from November 1980 showing complicated swirls, plumes, and fronts that marked the confluence of cold California Current water from the north, warm California Current water from the south, and cold upwelled water from near the coast. A relatively persistent anticyclonic eddy with a diameter of approximately 150 km has been reported to be centered near (32°N, 124°W) (Simpson *et al.*, 1984), not far from the beginning of FLIP's drift track. Bernstein *et al.* (1977) observed an intrusion of warm water into this area during February–March 1975. A search of the satellite infrared imagery available during this experiment was made at the Scripps Satellite Oceanography Facility. No completely cloud free images were found to illustrate the spatial variability of the sea surface temperature field along FLIP's drift track. Cloud free

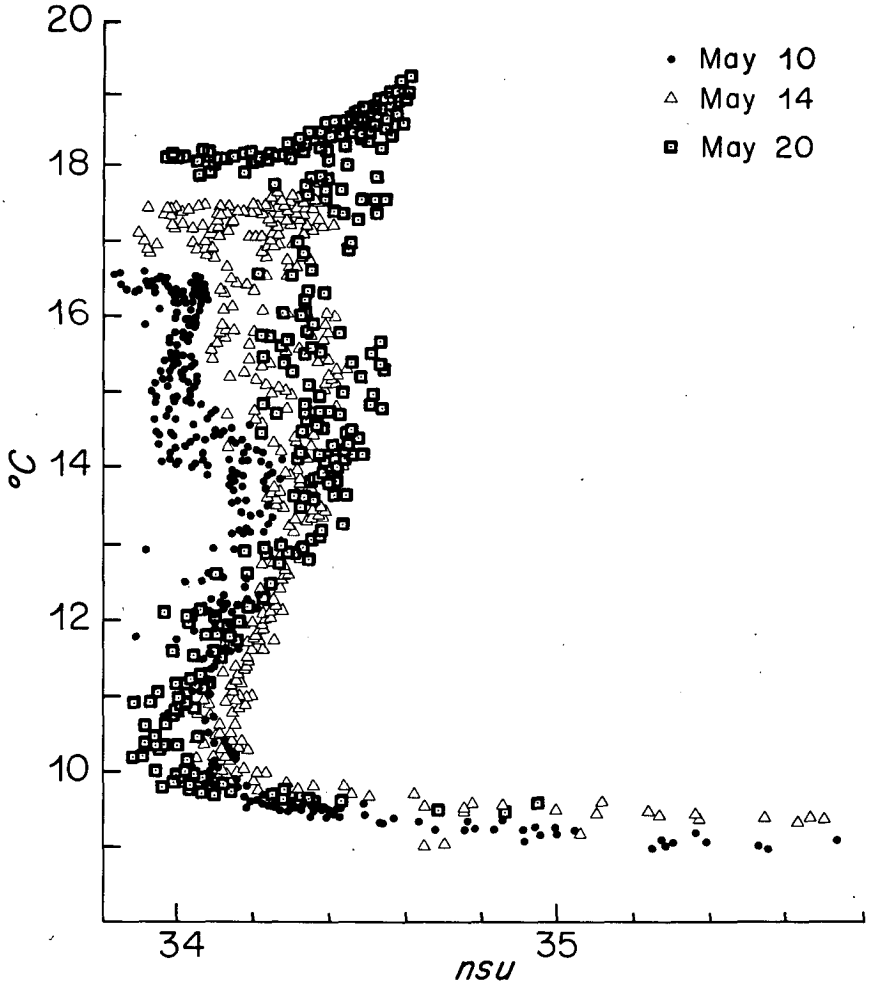

FIG. 4b. TS relations from three days of CTD data. The water encountered on 14 May as well as that encountered on 19–20 May was saltier as well as warmer.

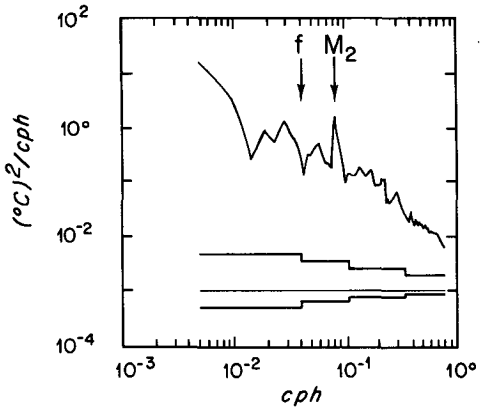

FIG. 5. Autospectrum of temperature at 130 m. The 95 percent confidence limits are shown.

images from an area directly to the east did, however, show swirls and plumes of cold water extending from the coast toward the region of the experiment and warm intrusions extending coastward from the vicinity of FLIP's drift track. Because the changes of temperature observed from FLIP (Fig. 4a) coincided with changes in salinity (Fig. 4b) and changes in the speed and direction of the absolute horizontal velocity (Fig. 6) and based on other work in the same region, it is believed that FLIP drifted through velocity and density fields marked by fronts and other variability associated with the California Current system.

To examine the vertical structure of the horizontal velocity field, velocity time series at various reference levels were subtracted from those at shallower depths. Figure 7, for example, shows a composite of progressive vector diagrams of flow at various depths relative to that at 106 meters. At subinertial frequencies the flow between 74 and 150 m was depth independent. Between 5 and 70 m there was a mean vertical shear; nearer the surface, the flow was both stronger and directed further to the south.

The relative flow observed in the upper 70 m at subinertial frequencies could to a large extent be successfully interpreted as an additional component of the velocity field found only the mixed layer and driven by the local wind. As seen in Fig. 7, the flow was directed to the right of the wind stress and veered further to the right and decayed with increasing depth. The mean flow at 5 m relative to 106 m was to be southwest and had an amplitude of approximately (130 km/26 day) or 6 cm s^{-1}. The mean flow at 22 m relative to 106 m was to the west and had an amplitude of approximately (90 km/26 day) or 4 cm s^{-1}. At 62 m the mean flow relative to 106 m was toward the north. Because the depth of the mixed layer was typically above 50 m, the relative transport in the upper 50 m was compared to the Ekman transport predicted from the observed wind; the transport computed relative to 50 m was within 1.5 percent of the magnitude of the predicted Ekman transport and directed 19 degrees further to the north.

The large amplitude oscillations seen at all depths in Figs. 3b and c were the dominant signal in the

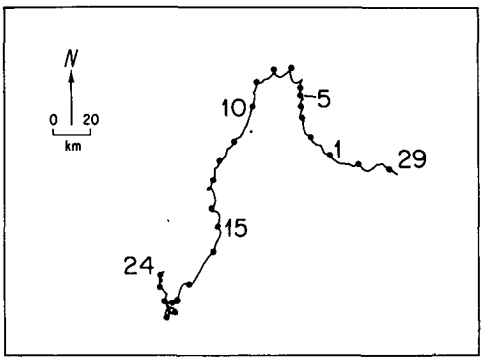

FIG. 6. Progressive vector diagram of the absolute horizontal velocity at 118 m.

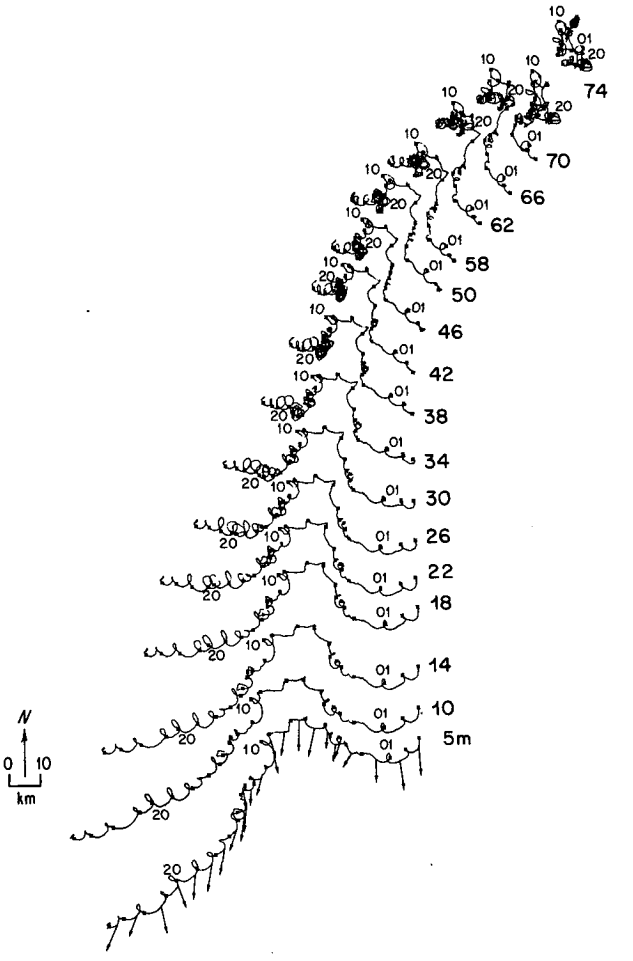

FIG. 7. A composite of progressive vector diagrams of flow at various depths relative to that at 106 m. Daily-averaged wind vectors are plotted at midday on the progressive vector diagram of the flow at 5 m relative to 106 m.

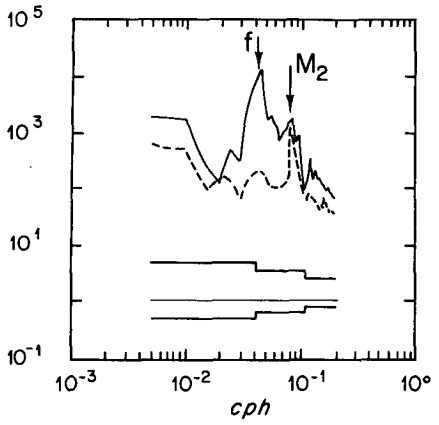

FIG. 8. Rotary autospectrum of the absolute horizontal velocity at 130 m. The solid line is the spectrum of the clockwise rotating components; the dashed line is the spectrum of the counterclockwise rotating components. 95 percent confidence limits are shown.

velocity field. Absolute amplitudes of these oscillations were as high as 40 cm s^{-1}. Figure 8 shows a representative rotary autospectrum of velocity; there is a prominent peak in the clockwise spectrum roughly centered at the local inertial frequency (f at 30°N is 0.0417 cph). This strong oscillatory motion is the focus of the following sections.

4. Velocity variability in the near-inertial frequency band

As mentioned above, the dominant feature of the relative and absolute horizontal velocity time series was the large amplitude oscillatory motion with the period of close to 24 hours and, for the range of latitudes over which FLIP drifted, close to the local inertial period. Rotary autospectra of the velocity time series showed that the oscillatory motion was nearly circular, rotated clockwise, and had a relatively sharp spectral peak (Fig. 8). The data was band-pass filtered, passing the band of 0.030 to 0.064 cph. This relatively broad pass band was chosen: 1) in order to ensure that the resulting time series would include all inertial and near-inertial motions measured from FLIP even though it drifted from 30°58'N (f = 0.043 cph) to 28°42'N (f = 0.040 cph) and even though, due to horizontal shear and/or stratification and to Doppler shifting associated with FLIP's motion, the frequency of the oscillations may have shifted from the local inertial frequency; 2) because no nearby spectral peaks were found that needed to be excluded; and 3) because the choice of a broad pass band minimized both the loss of data at the beginning and end of the time series and the smearing in time associated with the ringing of the filter. The filtered velocity data are shown in Figs. 9a and b. Note that a 5-hour running mean was applied before generating Figs. 9a and b in order to make them comparable with Figs. 3b and c. Peak amplitudes of the near-inertial velocities were, before smoothing, as high as 40 cm s^{-1}.

Because FLIP operated in the vicinity of 30°N, it is difficult to separate velocity variability associated with inertial motions caused by impulsive forcing or near-inertial internal waves from velocity variability associated with the 24-hour tides. In the region southwest of San Diego counterclockwise rotating semidiurnal tidal currents have amplitudes large compared to those of the diurnal tidal currents (Munk *et al.*, 1970), and the amplitude of the baroclinic semidiurnal tidal velocities found during the experiment (Pinkel, 1983) did not approach the size of the observed 24-

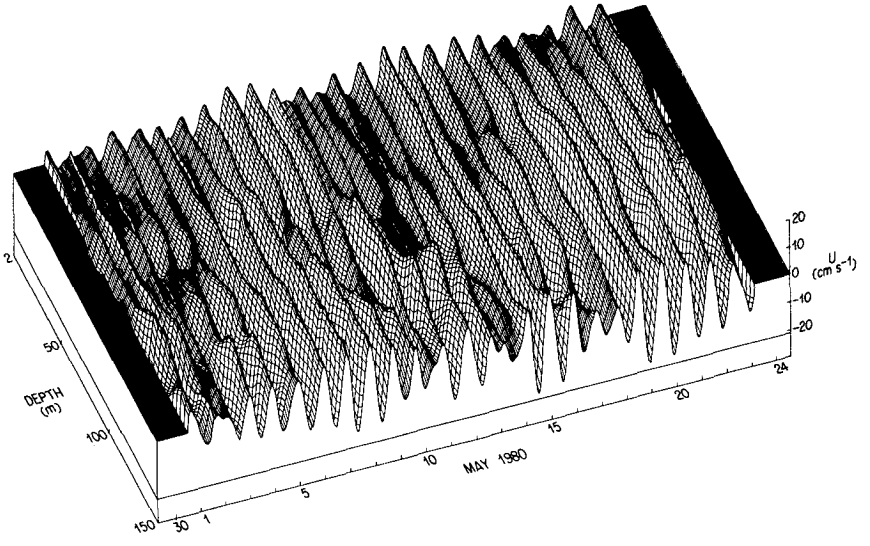

FIG. 9a. The u component of the near-inertial absolute velocity field. In order to match Fig. 3a a 5-hour running mean was applied before plotting.

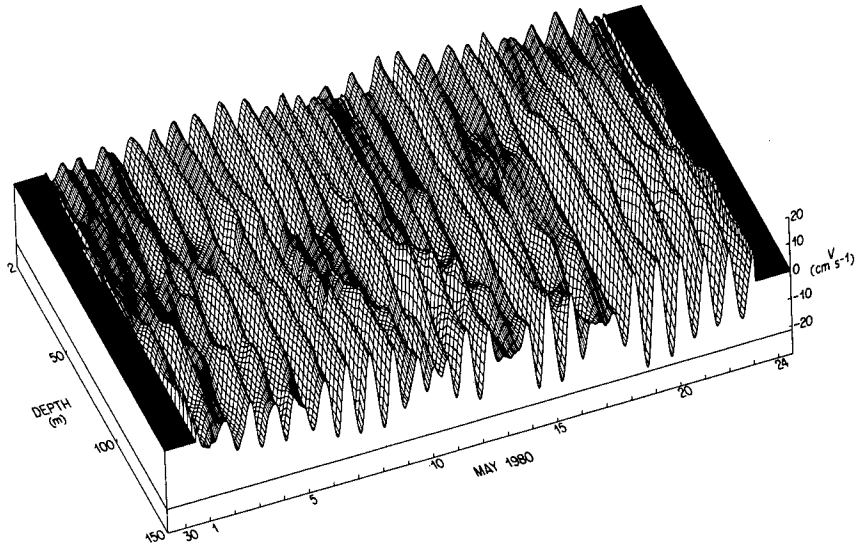

FIG. 9b. The v component of the near-inertial absolute velocity field. In order to match Fig. 3b a 5-hour running mean was applied before plotting.

hour oscillations. It is possible that a baroclinic component of the diurnal tide was present. Conversion of barotropic diurnal tidal motion into baroclinic inertial period motion by scattering off bottom topography is possible at 30°N, but would lead to oscillations of no more than 10 cm s^{-1} in magnitude at the surface (Hendershott, 1973). Thus, the 24-hour period oscillations are not thought to be tide-related.

The inertial oscillations appear (Figs. 9a and b) to have relatively large vertical scales of motion compared to the depth of the mixed layer. To examine the distribution of the variability among different vertical scales, and to decompose the fields into modes that could be examined for evidence of phase propagation with depth, the empirical orthogonal eigenfunctions of the band-passed velocity field were calculated. Ninety-seven percent of the velocity variability was associated with the first five vertical functions or modes (Fig. 10). EOF1 has the largest vertical scale and accounts for 79 percent of the total variability. If, below 150 m, the velocity vectors associated with this mode continued to rotate with depth at the rate found between 75 and 150 meters, the vertical wavelength of this mode would be approximately 600 meters. EOF2 (10 percent of the variability) shows a vertical wavelength below the mixed layer of approximately 90 m. EOF3 (5 percent) shows a vertical wavelength of approximately 56 m. EOF4 (2 percent) and EOF5 (1 percent) had vertical wavelengths of approximately 60 and 64 m, respectively. It cannot, of course, be assumed that the vertical structure of the inertial motion does not vary with depth. Below the mixed layer the vertical scales and horizontal velocities in the near-inertial band vary with depth as $N^2(z)$ varies. This depth dependence has been described by Leaman and Sanford (1975) and others. It is apparent, however, that the vertical scale of the energetic component of the near-inertial motion was large compared to the depth of the mixed layer.

EOF1, EOF2, and EOF3 are structured so that the horizontal velocity vector rotates clockwise with increasing depth, while in EOF4 and EOF5 the vectors rotate counterclockwise with increasing depth. Clock-

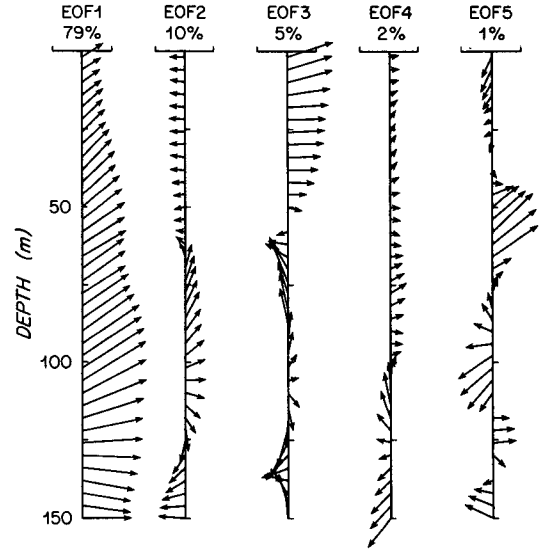

FIG. 10. The five empirical orthogonal functions (EOFs) with the largest percentages (as shown) of velocity variability in the near-inertial frequency band. The arrows represent horizontal velocity vectors. The vectors rotate clockwise with increasing depth in EOF1, EOF2, and EOF3. They rotate in the opposite direction in EOF4 and EOF5.

wise rotation with depth is, in the stratified region beneath the mixed layer, an indication of upward phase propagation and downward energy flux in the near-inertial band (Leaman and Sanford, 1975). The temporal variability of the amplitude of each of the first three eigenfunctions was computed. The product of that amplitude and the vector from a given depth of the associated eigenfunction gives the temporal variability of the component of the velocity field associated with that vertical mode at that depth. In the mixed layer (Fig. 11) the three modes have similar sizes. At 100 m (Fig. 12) EOF1 dominates the near-inertial velocity field.

Additional velocity information was obtained during the experiment in the region between 50 and 700 m by Dr. R. Pinkel's (Scripps Institution of Oceanography) Doppler sonars which were mounted on the hull of FLIP. Because Pinkel's data provides a description that complements that given above some of his findings are summarized here; for more detail see Pinkel (1983). The Doppler sonars were aimed out and down from FLIP. Each sonar provided a series of measurements, at roughly 20 m range intervals, of the velocity component along the beam. Velocity data from the sonars were, at ranges close to FLIP,

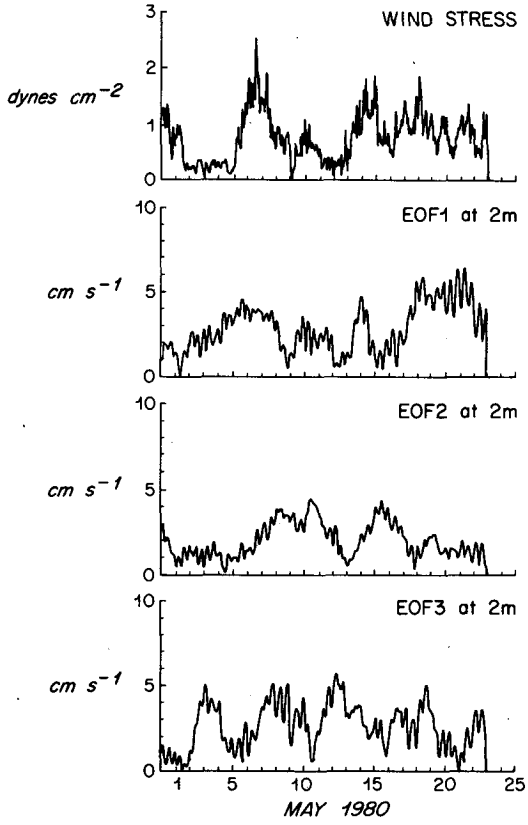

FIG. 11. Time series of wind stress and of the amplitude at 2 m of the velocity components associated with the three most energetic EOFs.

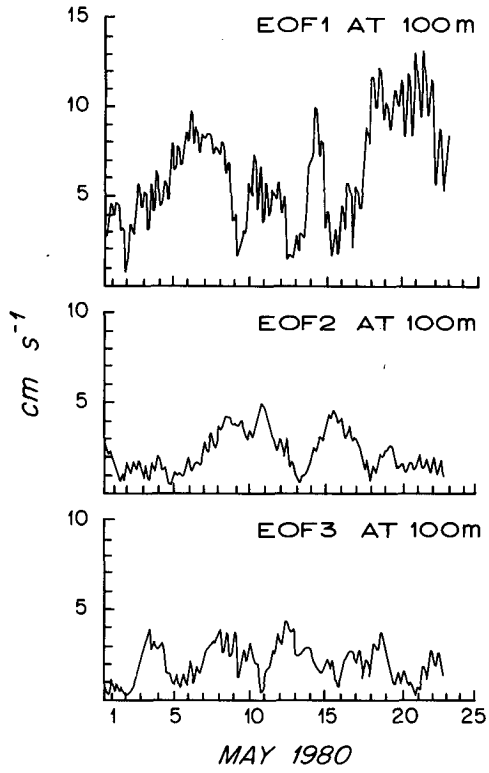

FIG. 12. Time series of the amplitude at 100 m of the velocity components associated with the three most energetic EOFs.

compared to the VMCM data and found to be in good agreement. The same energetic near-inertial motions found by the VMCMs in the 2–150 m depth range were also observed by the Doppler sonars in the 50–700 m depth range. In the VMCM data shown in Figs. 9a, b particularly energetic oscillations extend from 2 to 150 m on 5–9 May. In the Doppler sonar data, on 5–8 May, an energetic downward propagating group of near-inertial waves with a vertical wavelength of approximately 500 m was observed in the upper 200 m. In both data sets amplitudes peaked again on 11–12, 15–17, and 19–22 May. Downward propagating waves, observed by the Doppler sonar in the upper 200 m from 7 May through 22 May, the end of the Doppler record, had a vertical wavelength of approximately 125 m. The 500 and 125 m vertical wavelengths reported by Pinkel (1983) for the energetic, downward propagating wave groups are similar to the 600 and 90 m vertical wavelengths estimated for the two most energetic EOFs of the current meter data. On 11 May a less energetic upward propagating group, with a vertical wavelength of approximately 225 m was observed at extreme range in the Doppler data. After 16 May this group was no longer observed; it never penetrated above 400 m and thus was not observed by the VMCMs.

Pinkel (1983) performed rotary spectral analysis of the Doppler sonar velocity data after dividing it into

two pieces, 4–11 May and 13–22 May. In both time periods the results showed on average, at near-inertial frequencies, upward phase and thus downward energy propagation. This is consistent with the vertical structure of the dominant empirical orthogonal functions of the current meter data and confirms that energy was at, near-inertial frequencies propagating down from near the surface to depths of greater than 500 m.

5. Possible sources of the inertial motion

The dominance of downward energy (upward phase) propagation at near-inertial frequencies in near-surface velocity data has typically been taken to indicate the presence of a surface or near-surface source for and local generation of the near-inertial oscillations. Such local generation may be caused by disturbing existng steady wind-driven or geostrophic flows. Oceanic response to local forcing has been modeled, and the model predictions are typically in good agreement with observations of near-surface near-inertial response. For example, propagating patterns of wind stress curl, such as hurricanes, disturb the flow at depth as well as near the surface and thus are capable of creating strong inertial motions with vertical scales large compared to the depth of the mixed layer; Price, (1984) has found model predictions of upper ocean response to hurricanes to be in good agreement with observations. Typically, there is curl in the wind field off Baja California in the vicinity of the experiment (Hickey, 1979), but not of the strength or moving with the rapid translational speed of a hurricane. For the period of the experiment the National Weather Service 6-hour weather maps with ship reports from the region surrounding the area of the experiment were examined. No strong small scale wind events were reported, and FLIP's wind data were consistent with the synoptic meteorology. The observed motions are not thought to be generated by spatial variations in the wind.

Rapid changes in the magnitude or direction of the local wind stress are also effective at disturbing flow in the mixed layer and thus at generating inertial motions both there and, as smaller amplitude propagating near-inertial internal waves, in the region below (Pollard, 1970; Kundu, 1976; and Pollard, 1980). Time series of wind stress were computed from the observed wind using the Large and Pond (1982) speed dependent formulation for the drag coefficient. Used in the model of Pollard and Millard (1970),

$$\left.\begin{aligned} u_t - fv &= T^x/\rho H - cu \\ v_t + fu &= T^y/\rho H - cv \end{aligned}\right\}, \qquad (1)$$

with H, the observed mean mixed layer depth, and c, a damping coefficient equal to (96 hours)$^{-1}$, the observed wind stress, (T^x, T^y), can be used to predict slablike mixed layer inertial motions with a maximum amplitude of only 5 cm s^{-1}.

During the experiment heating was strong enough relative to wind mixing to produce diurnal variation in the depth of the mixed layer. In this case the use of the mean mixed layer depth in the slab model (1) may underestimate the near-surface near-inertial response. As well, the diurnal cycling of the buoyancy flux is in itself another source of near-inertial period variability (Fig. 13) not included in (1). The magnitude of the inertial response within the diurnal mixed layer was determined both by predicting the response using a model that included both buoyancy and momentum fluxes (Price *et al.*, 1985) and by carefully examining the flow unique to the diurnal mixed layer. Model predictions and data showed inertial motions confined to the mixed layer that had amplitudes of at most 6 cm s^{-1}.

Thus, though the observed upward phase propagation suggested a near-surface source for the large amplitude near-inertial motion, local meteorological forcing alone cannot directly explain the strength and variability of the observed, energetic near-inertial velocity variability.

A theoretical study by Stern (1977) and results from Weller (1982), Kunze and Sanford (1984) and Kunze (1984) show that the amplitude of the near-surface near-inertial motion is also influenced by the vertical and horizontal shear, respectively, of the quasi-geostrophic flow field. There was mean vertical shear in the upper 70 m (Fig. 7). There was, in addition, mean vertical shear across the main thermocline; flow in the upper 150 m was 5 cm s^{-1} toward the south relative to the bottom, and the flow in the layer between 200 and 550 m was 2 cm s^{-1} toward the west relative to the bottom (Pinkel, 1983). Such vertical structure is consistent with other descriptions of the flow in the California Current system (Hickey, 1979, and Simpson *et al.*, 1984). Significant horizontal shear, associated with fronts and other features, has also been observed in this region. In the eddy surveyed by Simpson *et al.* (1984) in the fall of 1980 the horizontal shear of horizontal velocity was as high as approximately (30 cm s^{-1}/30 km) or 1×10^{-5} s^{-1}.

Stern (1977) showed that a near-inertial wave that propagated upward and upwind through a vertical shear could be amplified when it reflected off the base of the mixed layer. If that wave then reflected back upward again and the process repeated itself again and again until an equilibrium was reached, then strong near-inertial oscillations would be present in and below the mixed layer even though the wind forcing was moderate. However, these motions would according to Stern (1977), for the conditions observed from FLIP, have a horizontal wavelength of approximately 75 km. This was not the case; Pinkel's (1983) estimates of the horizontal wavelengths of the two

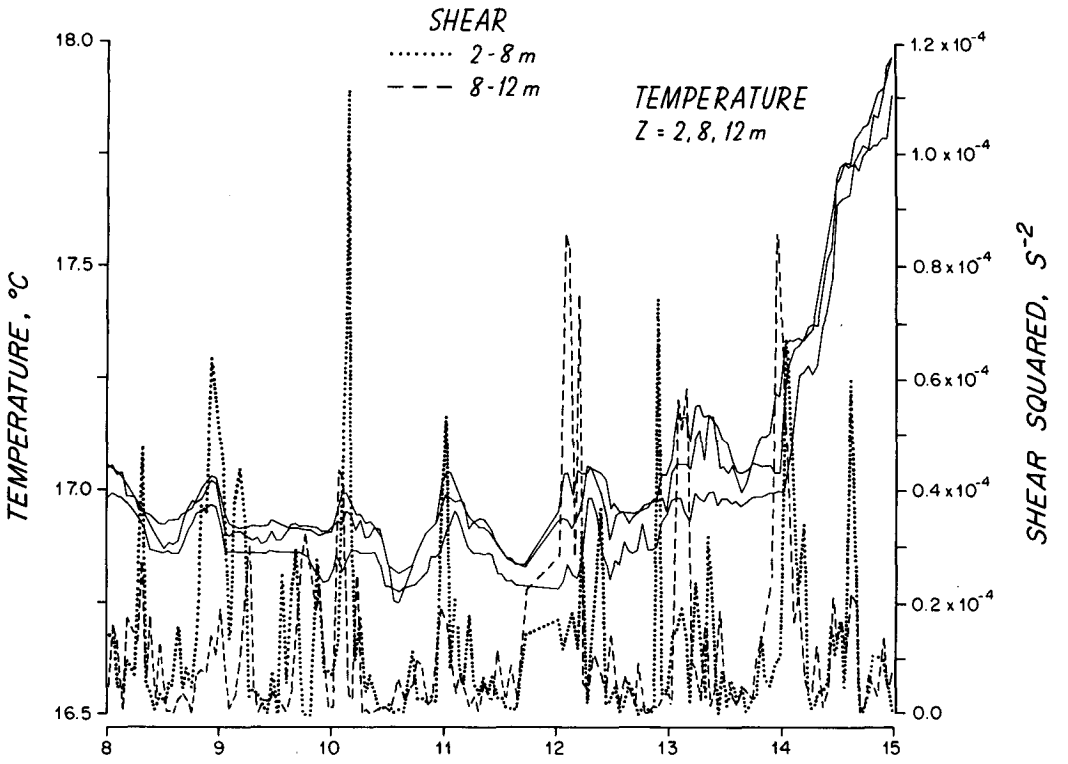

FIG. 13. Time series of temperature at 2, 8, and 12 m (solid lines) and of the vertical shear of the horizontal velocity computed between 2 and 8 m and between 8 and 12 m. As the diurnal mixed layer warmed in response to the solar radiation and then deepened later in the day the VMCMs recorded a temperature increase of several tenths °C and a sharp, short-lived rise in the vertical shear of the horizontal velocity as the base of the mixed layer deepened past the depth of each instrument. The velocity and temperature data used to produce these plots were 6-minute averages; this averaging suppressed high frequency variability associated with surface and internal waves. The VMCM temperature sensors could not be calibrated precisely and showed offsets even when the shear dropped and the CTD data confirmed that the mixed layer was isothermal.

downward propagating near-inertial groups were 8.5 and 25 km. As well, the EOF analysis did not show, near the surface, evidence of both upward and downward propagating wave groups of similar strength.

These relatively small horizontal scales (8.5 and 25 km) and the temporal variability of the amplitude of the near-inertial motion both more nearly matched the horizontal scales and variability of the fields through which FLIP drifted. Time series of the magnitude of EOF1, which represents 79 percent of the near-inertial variability, showed amplitude increases immediately preceding and during rapid changes in temperature on 3–8, 13.5–14.5, and 18–22 May (Fig. 14). Increases in the amplitude of EOF2, which represents another 10 percent of the variability, occurred on 6–12 and 14–17 May (see Fig. 11), just after increases in temperature.

It should be noted that Fig. 14 emphasizes temporal variability. Differences in the abruptness of the increase in both temperature and the amplitude of EOF1 in this plot are due to differences in FLIP's drift velocity. FLIP's drift speed was largest on 14 May, smallest on 5–8 May. The distances over which FLIP drifted while both temperature increased and near-inertial amplitudes were elevated were similar, 18, 20, and 25 km for the three periods, respectively, and close to the horizontal scales estimated by Pinkel (1983).

Another period of elevated amplitude, 9.5–12 May, was not, however, associated with a large temperature change. In Fig. 15 the temporal and spatial variability of the temperature and also the absolute velocity fields have been combined. The periods marked ***a***, ***b***,

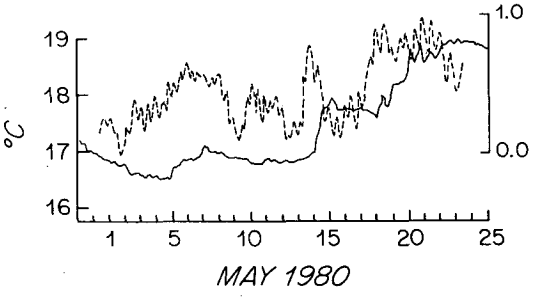

FIG. 14. Time series of the dimensionless amplitude of EOF1 (dashed line) superimposed upon the time series of temperature at 22 m (solid line).

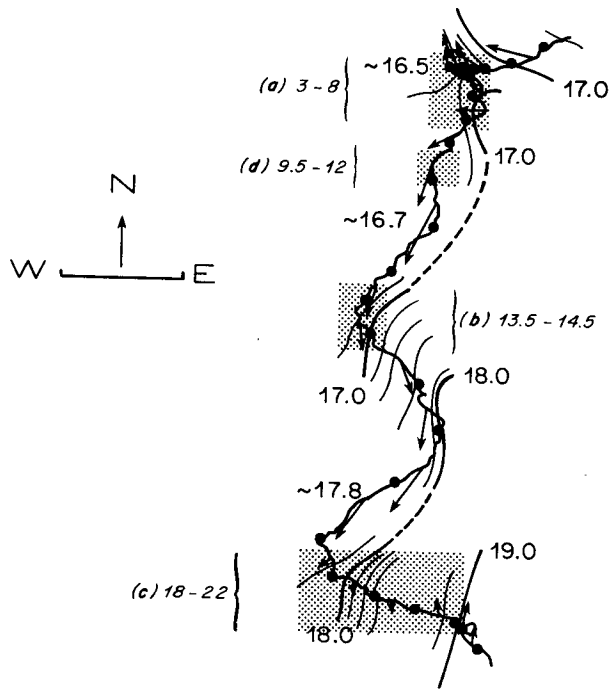

FIG. 15. FLIP's drift track. The length of the east–west line and of the north arrow correspond, respectively, to distances of 20 km in the east–west and north–south directions. Daily-averaged absolute velocities from 118 m have been drawn with their tails located at the noon position of each day; an arrow of the length of the north arrow in the scale would correspond to a velocity of 15 cm s^{-1}. Temperature isolines have been drawn in based on the mixed layer temperatures observed from FLIP. Four periods of elevated near-inertial variability are marked with stippling and labelled ***a***, ***b***, ***c***, and ***d***.

and ***c*** correspond to the three times when both the amplitude of EOF1 and the temperature increased. The period marked ***d*** is the time, 9.5–12 May, when the amplitude was elevated but the temperature did not increase. Along the drift track there was considerable spatial variability in horizontal velocity as well as in temperature; and all four periods of elevated near-inertial amplitudes coincide with regions of horizontal shear, suggesting that the link is between the subinertial and near-inertial flow fields.

Weller (1982) found that the presence of horizontal gradients in the quasi-geostrophic flow field introduced variability in the amplitude of wind-driven inertial motion in the mixed layer. This effect was modeled with the following equations:

$$\left.\begin{aligned} u_t - fv + U_x u + U_y v &= T^x/\rho H \\ v_t + fu + V_y v + U_x u &= T^y/\rho H \end{aligned}\right\}, \tag{2}$$

where the velocities are depth averages over the depth of the mixed layer with (u, v) being the wind-driven flow and (U, V) the quasi-geostrophic flow. Where $(U_x + V_y) \ll f$ and $(V_x - U_y) \ll f$ the homogeneous solution of the equation is

$$\left.\begin{aligned} u &= u_0 \exp[-\tfrac{1}{2}(U_x + V_y)t] \\ &\quad \times \sin\{f[1 + (V_x - U_y)/2f]t\} \\ v &= v_0 \exp[-\tfrac{1}{2}(U_x + V_y)t] \\ &\quad \times \cos\{f[1 + (V_x - U_y)/2f]t\} \end{aligned}\right\}. \tag{3}$$

The divergence of the quasi-geostrophic flow causes exponential growth or decay in the amplitude of inertial motions generated by the local wind, and the vorticity of the quasi-geostrophic flow field shifts the frequency of the free inertial oscillations.

Equations (3) show how the motion in the mixed layer might be modified; they do not explain the interaction of the near-inertial internal waves below the base of the mixed layer with the horizontal shear. Kunze (1984) retained the terms of the form Uu_x and uU_x in the equation of motion while deriving an approximate dispersion relation for near-inertial internal waves. He found the effects of stratification and vertical shear on the propagation of near-inertial internal waves to be small compared to the effects caused by background vorticity shifting the effective inertial frequency, $f_{\text{eff}} = f + \frac{1}{2}(V_x - U_y)$. The most striking effect is that near-inertial internal waves generated in a region of negative vorticity remain trapped within that region. This finding allowed Kunze and Sanford (1984) to explain an intensification of near-inertial wave energy found on the warm, western edge of a front. The front had an associated southward flowing jet. In the western part of the jet V_x was negative and f_{eff} smaller than elsewhere; near-inertial internal waves generated within this region were trapped there, resulting in localized intensification of near-inertial velocities.

Assuming that the subinertial field through which FLIP drifted was fixed, the daily-averaged velocities and daily positions were used to examine the variability of the vorticity, $(\Delta V/\Delta x - \Delta U/\Delta y)$, along the drift track. Because the field was not fixed and because its spatial variability could only be crudely reconstructed from the FLIP data, these values were taken only as indicators of the sign and approximate magnitude of the vorticity of the quasi-geostrophic flow field. The daily estimates ranged between -15×10^{-5} s^{-1} and 11×10^{-5} s^{-1} [Simpson *et al.* (1984) reported the vertical component of the relative vorticity associated with the eddy they observed in this region to be -4×10^{-5} s^{-1}], of the same magnitude as f and thus able to significantly change f_{eff}. (Kunze, 1984, found trapping in ray tracing experiments when the change was only ten percent.)

The estimates of vorticity were negative on 29 April, 4, 6, 9–10, 14–16, 18–19, and 21 May. To be consistent with the trapping mechanism demonstrated by Kunze's (1984) ray tracing experiments the energetic near-inertial motion should be found only within

the region of negative vorticity. The four periods of observed energetic near-inertial motion discussed above, 3–8, 9.5–12, 13.5–14.5, and 18–22 May (partial days indicated in tenths), do indeed approximately coincide with the dates when the estimated vorticity was negative. The near-inertial motions were most energetic at approximately 250 m and were concentrated in the upper 350–400 m (Pinkel, 1983). This vertical structure matches the vertical structure of the mean flow found during the experiment and that reported for the California Current system (Hickey, 1979; and Simpson *et al.*, 1984) and thus also matches the probable vertical extent of the region of negative vorticity.

Thus, trapping of near-inertial internal waves within regions of negative vorticity and reflection of the waves away from regions of positive vorticity lead to a near-inertial velocity field in the California Current system that was highly variable in space and, in locations, more energetic than anticipated. The trapping mechanism does not, however, provide an explanation of the initial source of the motion. If the sheared, frontal regions encountered by FLIP had associated convergent surface flow, as has been observed at the subtropical front in the Pacific (Niiler and Reynolds, 1984), then the wind-driven mixed layer inertial motion in those locations would as well have been amplified as shown by Eq. (3) (Weller, 1982). That inertial motion would then be an effective source, as discussed by Kroll (1975) and others, for downward propagating near-inertial internal waves. These downward propagating waves would then be trapped and concentrated within the negative vorticity regions of the quasi-geostrophic flow field and reflected away from the positive vorticity regions. Even without convergent surface flow, some level of inertial motion would be present in the mixed layer as suggested by predictions based on the observed wind and the Pollard and Millard (1970) and Price *et al.* (1985) models. Because only near-inertial internal waves generated within the region of negative vorticity can be trapped and intensified there, it is probable that the source of the energetic near-inertial motion observed from FLIP was, indirectly, the wind.

6. Conclusions

Upper ocean velocity measurements were made from the Research Platform FLIP off the coast of Baja California. At subinertial frequencies the observed flow had two components. One was the spatially varying velocity field associated with the California Current system. The second component was driven by local atmospheric forcing, was found only in the mixed layer, which had an average depth of 50 m, and was superimposed upon the first. The detailed vertical structure of this atmospherically forced velocity field was determined by both the wind forcing and the heating; but, on average, the flow veered to the right, decayed with depth, and had a transport close to the predicted Ekman transport.

In contrast, at near-inertial frequencies only a small component of the observed variability found in the mixed layer and directly below was predictable from the local wind. Energetic oscillations found throughout the upper 150 m that had vertical scales large compared to the depth of the mixed layer dominated the velocity field in the near-inertial band. These near-inertial waves were downward propagating. Because the most energetic oscillations encountered during FLIP's drift were found in association with regions of horizontal shear in the larger scale, subinertial flow field, it is believed that local intensifications of near-inertial energy caused by regions of negative vorticity, as previously described by Kunze (1984), were encountered. If the subinertial flow in these regions was also convergent, then the wind-driven mixed layer inertial motions may, as observed in JASIN 1978 (Weller, 1982), have been amplified above the level produced by the wind alone and thus have provided a good source of the near-inertial internal waves trapped in the regions of negative vorticity.

Kunze (1984) suggests that variability in near-inertial amplitudes associated with regions of negative vorticity is not uncommon. In addition to the mid-Pacific front (Kunze and Sanford, 1984) he reports finding such variability in the upper ocean in warm core rings, a Gulf Stream cold core ring, and at the edge of an anticyclonic eddy over a seamount. Past measurements might also be reinterpreted. Tang (1979) had noted the coincidence of strong inertial motion with rapid veering or acceleration of the subinertial frequency component of the flow in moored current meter data from the Gulf of St. Lawrence. He had interpreted the data as evidence of a transient current that was unbalanced and that during the process of geostrophic adjustment was the source of inertial motion. Some of the veering events reported by Tang (1979) had large, coincident temperature changes. An alternative explanation is that the fixed current meters observed temperature changes and veering as the relatively sharp boundaries of a quasi-geostrophic feature, such as a front or an eddy, were advected past the moorings by the large scale flow field. The boundary regions were potentially areas of negative vorticity and thus of trapping of near-inertial internal waves. Those areas, like the regions encountered by FLIP, would be characterized by large near-inertial velocities.

During the FLIP experiment no evidence was collected that suggested that the observed energetic near-inertial motion played an important role in the dynamics of the mixed layer response to atmospheric forcing. The presence of the large vertical scale near-inertial oscillations did not affect mixed layer response, presumably, because there was little shear across the

base of the mixed layer associated with these motions. Future experiments, where the horizontal and vertical velocity, the temperature, the density, and the meteorological fields will be more adequately mapped, are planned for frontal regions in order to more thoroughly investigate the processes and dynamics discussed in this paper.

Acknowledgments. This research was supported by the Office of Naval Research through Contracts N00014-75-C-0152 with the University of California, San Diego and N00014-76-C-0197, NR083-400 with the Woods Hole Oceanographic Institution. The assistance of Drs. Russ Davis and Rob Pinkel of Scripps Institution of Oceanography made the preparation for and execution of the experiment possible. Discussions of the data with Rob Pinkel and Jim Price are gratefully acknowledged as is the use of data collected by Rob Pinkel. Interaction with Eric Kunze in the form of ideas and manuscripts exchanged was an essential element in progressing toward an understanding of the observed near-inertial motion. The efforts of Jim Parks, Steve Wald, Bill Powell, and Eric Slater in preparing the equipment and at sea are gratefully acknowledged as are the efforts of Nancy Pennington and Erika Francis during the analysis of the data. Kathy Kelly supplied several satellite infrared images of the area of the experiment, and David Mountain obtained the 6-hourly weather maps. The crewmembers of R.P. FLIP are thanked for their cheerful assistance.

REFERENCES

Bernstein, R. L., L. Breaker and R. Whritner, 1977: California Current eddy formation: Ship, air, and satellite results. *Science,* **195,** 353–359.

Davis, R. E., and R. A. Weller, 1980: Propeller current sensors. *Air–Sea Interaction: Instruments and Methods,* F. Dobson, L. Hasse and R. Davis, Eds., Plenum, 141–154.

Hendershott, M. C., 1973: Inertial oscillations of tidal period. *Progress in Oceanography,* Vol. 8, Pergamon, 191–279.

Hickey, B., 1979: The California Current System—hypothesis and facts. *Progress in Oceanography,* Vol. 8, Pergamon, 191–279.

Kroll, J., 1975: The propagation of wind-generated inertial oscillations from the surface into the deep ocean. *J. Mar. Res.,* **33,** 15–51.

Kundu, P. K., 1976: An analysis of inertial oscillations observed near the Oregon coast. *J. Phys. Oceanogr.,* **6,** 879–893.

Kunze, E., 1985: Near-inertial propagation in geostrophic shear. *J. Phys. Oceanogr.* (in press).

——, and T. B. Sanford, 1984: Observations of near-inertial waves in a front. *J. Phys. Oceanogr.* **14,** 566–581.

Large, W. G., and S. Pond, 1982: Sensible and latent heat flux measurements over the ocean. *J. Phys. Oceanogr.,* **12,** 879–893.

Leaman, K. D., and T. B. Sanford, 1975: Vertical energy propagation of inertial waves: a vector spectral analysis of velocity profiles. *J. Geophys. Res.,* **80,** 1975–1978.

Lynn, R. J., and J. Svejkovsky, 1984: Remotely sensed sea surface temperature variability off California during a "Santa Ana" clearing. *J. Geophys. Res.,* **89,** 8151–8162.

Niiler, P. P., and R. W. Reynolds, 1984: The three-dimensional circulation near the eastern North Pacific subtropical front. *J. Phys. Oceanogr.,* **14,** 217–230.

Munk, W., F. Snodgrass and M. Wimbush, 1970: Tides off-shore: Transistion from California coastal to deep-sea waters. *Geophys. Fluid Dyn.,* **1,** 161–235.

Pinkel, R., 1983: Doppler sonar observations of internal waves. *J. Phys. Oceanogr.,* **13,** 804–815.

Pollard, R. T., 1970: On the generation by winds of inertial waves in the ocean. *Deep-Sea Res.,* **17,** 795–812.

——, 1980: Properties of near-surface inertial oscillations. *J. Phys. Oceanogr.,* **10,** 385–398.

——, and R. C. Millard, 1970: Comparison between observed and simulated wind-generated inertial oscillations. *Deep-Sea Res.,* **17,** 813–821.

Price, J. F., 1985: Internal wave wake of a moving storm. Part II: Parameter dependence. Submitted to *J. Phys. Oceanogr.*

——, R. A. Weller and R. Pinkel, 1985: Diurnal cycling: Observations and modelling of the upper ocean response to diurnal heating, cooling, and wind mixing. Submitted to *J. Geophys. Res.*.

Regier, L. A., 1975: Observations of the power and directional spectrum of oceanic surface waves. Ph.D. Thesis, University of California, San Diego, 176 pp.

Rudnick, P., 1967: Motion of a large spar buoy in sea waves. *J. Ship Res.,* **11,** 257–267.

Simpson, J. J., T. Dickey and C. J. Koblinsky, 1984: An offshore eddy in the California Current System. Part I. Interior dynamics. *Progress in Oceanonography,* Vol. 13, Pergamon, 1–49.

Stern, M. E., 1977: Interaction of inertia-gravity waves with the wind. *J. Mar. Res.,* **35,** 479–498.

Tang, C. L., 1979: Inertial waves in the Gulf of St. Lawrence: A study of geostrophic adjustment. *Atmos. Oceanic Phys.,* **17,** 135–156.

Weller, R. A., 1978: Observations of the horizontal velocity field in the upper ocean with a new vector measuring current meter. Ph.D. thesis, University of California, San Diego, 169 pp.

——, 1982: The relation of near-inertial motions observed in the mixed layer during the JASIN (1978) experiment to the local wind stress and to the quasi-geostrophic flow field. *J. Phys. Oceanogr.,* **12,** 1122–1136.

——, and R. E. Davis, 1980: A vector measuring current meter. *Deep-Sea Res.,* **27A,** 565–582.